

Minerals of a soil developed in the meteoritic crater of Carancas, Peru, and evidences of phase changes on the impact event

María L. Cerón Loayza · Jorge A. Bravo Cabrejos

© Springer Science+Business Media Dordrecht 2013

Abstract We report studies about the phase transformations in the soil of the Carancas meteoritic crater located in an inhabited area near the town of Carancas, in the Region of Puno, about 1,300 km southeast of Lima, Peru. The studies by energy dispersive X-ray fluorescence, X-ray diffractometry and transmission Mössbauer spectroscopy (at RT and 77 K) reveal that the sample consists mainly of quartz, albite and impactites such as coesite and stishovite (SiO_2) that have experienced phase metamorphism or alterations, related to high pressures and temperatures, forming their corresponding polymorphs. The occurrence of these phases, with high content of SiO_2 , in the soil of the crater strengthens the hypothesis of its origin by metamorphism induced by impact; we observed also a magnetic sextet on the Mössbauer pattern, assigned to the Fe^{3+} in hematite, and three paramagnetic doublets, two of them associated with structural Fe^{3+} and Fe^{2+} cations, respectively, in illite and/or montmorillonite, and a third one due to an unidentified Fe^{3+} site.

Keywords Transmission Mössbauer spectroscopy · X-ray diffractometry · X-ray fluorescence · Metamorphism · Coesite · Stishovite · Impactites

1 Introduction

Continuing with our previous studies of the Carancas meteorite [1] in Puno, Peru, we now present results related to studies of three soil samples collected from different

Proceedings of the Thirteenth Latin American Conference on the Applications of the Mössbauer Effect, (LACAME 2012), Medellín, Colombia, 11–16 November 2012.

M. L. Cerón Loayza (✉) · J. A. Bravo Cabrejos
Laboratorios de Análisis de Suelos y Arqueometría, Facultad de Ciencias Físicas,
Universidad Nacional Mayor de San Marcos, Apartado Postal 14-0149, Lima 14, Perú
e-mail: malucelo@hotmail.com

J. A. Bravo Cabrejos
e-mail: jbravo8@hotmail.com

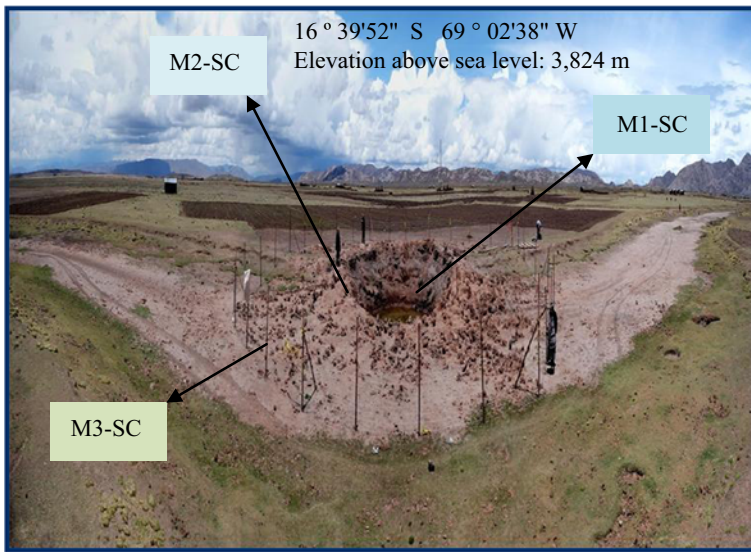


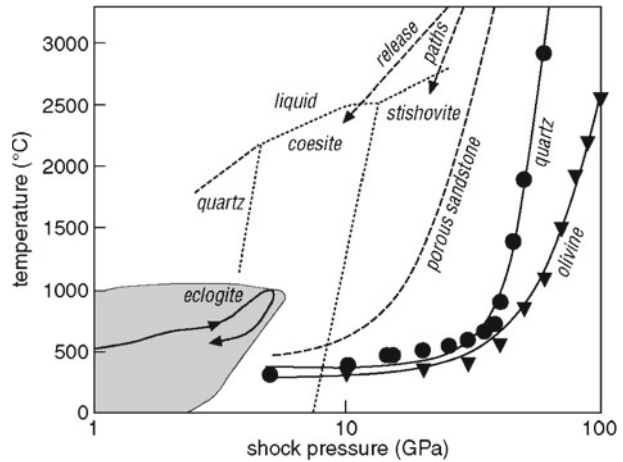
Fig. 1 The Carancas crater. It is shown the site positions from where the samples were collected (the photo was taken in November 2007)

positions within the crater as seen in Fig. 1 (located at $16^{\circ} 39'52''$ S, $69^{\circ} 02'38''$ W, 3,824 meters above sea level) which witness events of phase transformations. In general, minerals show a unique response when subjected to shock waves due to the occurrence of high pressures and temperatures. The effects caused by transforming them to other minerals are an unmistakable fingerprint of the impact event [2]. The metamorphic minerals may be regarded as a relic of the meteorite impact witnessing the age of the geological event.

A shock wave is a compression wave that propagates with supersonic velocity and abruptly affects compressing, heating and deforming plastically the solid matter. In the sense of an impact of a planetary body on the Earth surface, the shock waves are fundamentally different from seismic waves (elastic) [3]: the shock forms an internal compression wave that reacts almost instantly against an internal decompression wave that fractures the crust and projects pulverized materials into the atmosphere. At the instant of the impact, shock waves are generated from an abrupt increase of both pressure and temperature, drastically changing or virtually destroying the structure of rocks, leading to their fracture; the high temperature causes an impact metamorphism, by reforming minerals to generate new structures such as coesite y stishovite (high pressure modifications of SiO_2 , with the same composition of quartz but with a more compact structure). If the meteorite is sufficiently large, the rocks may even melt and vaporize. In Fig. 2, we see the phase diagrams of coesite and stishovite, which are minerals that have been found from this study.

The purpose of this work was to study the phase changes under metamorphism of soil minerals from samples collected from the meteoritic crater of Carancas in Puno, Peru, in an attempt to characterize the main structural properties of these samples applying the analytical techniques available in our Faculty of Physical Sciences-UNMSM, such as energy dispersive X-ray fluorescence (EDXRF), X-ray diffractometry (XRD) and particularly transmission ^{57}Fe Mössbauer spectroscopy

Fig. 2 Phase diagram depicting the pressure-temperature conditions reached in quartz, olivine (solid line), and porous sandstone (long dashed line) by shock compression (data after Wackerle [4], Kieffer et al. [5], Holland and Ahrens [6]). The release paths hold for porous quartz, which first melts on loading and then solidifies on cooling as coesite or stishovite. The equilibrium phase boundaries between quartz, coesite, stishovite and liquid are drawn as dashed lines



(TMS) for being an isotope selective technique. This meteorite impact caused a great explosion and formed a crater with approximately 20 m in diameter and 3 m in depth. At the site, the underground water table lies at a depth of about 3 m; therefore, the crater lies partially filled with water.

2 Materials and methods

The collection of the samples used in this study was undertaken two weeks after the meteorite impact that took place on September 15, 2007. These samples were obtained in collaboration with Dr. J. Itshitsuka, Instituto Geofísico del Perú, and were classified as:

- M1-SC: Sample from inside the crater, reddish color,
- M2-SC: Sample from the central part of the crater, grayish color, and
- M3-SC: Sample from outside the crater, brown color.

These materials were ground in an agatha mortar to a fine 160 μm mesh powder for analysis by XRD and TMS at RT; pellets were prepared for EDXRF analysis. The TMS spectra at 72 K were taken in collaboration with Dr. J.M. Grenech, Laboratoire de Physique de l'État Condensé, Université du Maine, Le Mans, France, using about 150 mg of each sample powder.

2.1 Analysis by Energy Dispersive X-Ray Fluorescence (EDXRF)

The elemental composition analysis was performed with a portable EDXRF AMPTEK instrument. This instrument uses an X-ray tube with an Ag anode operating at 30 kV and 30 μA . This instrument allows the identification of elements with $Z > 12$ (magnesium). Results of these quantitative analyses are given in Table 1. This was done by fitting the experimental EDXRF spectrum with a program that simulates EDXRF spectra based on the fundamental parameters model; this program is written in FORTRAN and simulates all physical processes that affect an X-ray spectrum: energy distribution of the primary and secondary radiation,

Table 1 Results from the quantitative elemental analysis of the studied samples compared to the meteorite elemental composition

Element	Samples Concentration (% weight)			
	Meteorite	M1-SC	M2-SC	M3-SC
Al	7.50	9.0	9.8	9.7
Si	13.0	27.0	21.2	24.0
S	0.90	0.01	0.01	0.01
Cl	0.90	0.70	0.47	0.76
K	0.35	1.43	1.36	1.05
Ca	0.66	0.92	1.37	3.46
Ti	0.04	0.38	0.30	0.37
Cr	0.11	0.09	0.01	0.01
Mn	0.12	0.10	0.07	0.12
Fe	6.00	3.39	1.69	3.30
Ni	0.22	0.01	–	0.01
Cu	–	0.06	0.04	0.06
Zn	0.01	0.07	0.06	0.08
La	0.10	–	–	–
Rb	–	0.01	0.01	0.01
Sr	–	0.01	0.05	0.02

propagation, scattering, absorption and photoelectric production, which take place in an EDXRF measurement with the used experimental geometry. It is based on data of X-ray cross sections provided by NIST and atomic characteristic X ray parameters provided by IAEA. The X-ray distribution function, which includes continuous and discrete components, has been calibrated by performing scattering of these primary X-rays by known samples. The performance of the program has been checked using reference samples. The estimated uncertainty in these measurements of the elemental concentrations is about 10 %, depending on the atomic number of the element (Dr. J.A. Bravo C., private communication).

2.2 Analysis by X-Ray Diffractometry (XRD)

For the structural analysis of the minerals present in the sample, the XRD technique was applied using a BRUKER diffractometer, model D8-Focus, with $\text{CuK}\alpha$ (1.5406 Å) radiation (40 kV, 40 mA) and a vertical goniometer. The scanned angle interval was $4^\circ < 2\theta < 90^\circ$ and the 2θ advance was $0.02^\circ/\text{step}$ with a time interval of 3 s per step.

2.3 Analysis by ^{57}Fe transmission Mössbauer spectroscopy (TMS)

TMS was used to obtain more detailed information about iron containing minerals. A conventional spectrometer was used with a sinusoidal velocity modulation signal and 1,024 channels. The Mössbauer spectrum at room temperature (RT: ~298 K) was collected at the Laboratory of Archaeometry, Facultad de Ciencias Físicas, UNMSM. TMS measurements at liquid nitrogen temperature (LNT; ~80 K) were collected at Laboratoire de Physique de l'État Condensé, Université du Maine, Le Mans, France.

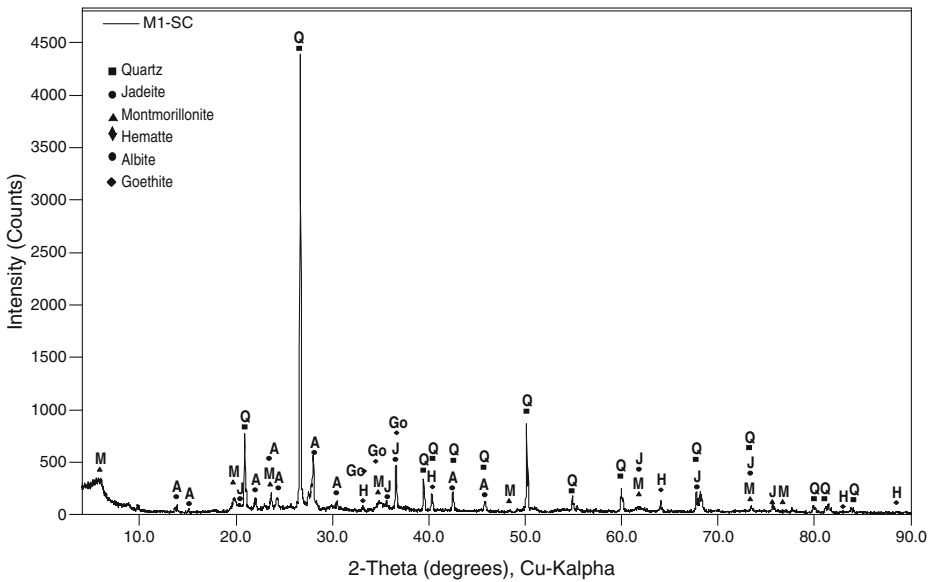


Fig. 3 X ray pattern for the sample M1-SC from the Carancas crater showing reflections of: Quartz (Q), Montmorillonite (M), Jadeite (J), Hematite (H), Albite (A) and Goethite (Go)

A ^{57}Co source in a Rh matrix was used to collect spectra, which were analyzed using the Normos program written by R. Brand (Normos Site) [7].

3 Results and discussion

Table 1 lists data from the quantitative elemental chemical analyses for the studied samples; for comparison it lists also data from the elemental composition of a sample of the Carancas meteorite whose elemental composition has already been reported [8]. The meteorite sample shows the presence of the following elements: Si, Cl, S, K, Fe, Cr, Cu, Ca, Ti, Mn, and Ni, with relatively high concentration of Fe, as well as of S, Cl, Cr and Ni, compared to soil samples from the crater. The soil samples do contain: Si, S, Cl, K, Ca, Ti, Mn, Fe, Ni, Cu, Zn, Rb, and Sr; Si, Ca, and Ti are present in higher concentrations compared to the meteorite; Ca is found in the following proportions $M3 > M2 > M1$; Fe as $M1 > M3 > M2$; and Zn and Mn as $M3 > M1 > M2$; the elements Al, S, Rb, Sr and Cu are present in about the same concentrations in the three samples. Ni is present only in samples M1-SC and M3-SC, but in low concentrations.

The diffractograms of Figs. 3, 4 and 5 are, respectively, for samples M1-SC, M2-SC and M3-SC. All of them show typical reflections of mineralogical phases that include mainly quartz (SiO_2), montmorillonite, illite, albite ($\text{NaAlSi}_3\text{O}_8$), and hematite. In samples M1-SC and M3-SC, montmorillonite has strong characteristic (0 0 ℓ) reflection peaks; the sample M2-SC shows a very strong characteristic (0 0 1) peak of illite. The reflection peaks of hematite appear to correspond to a well crystallized mineral in samples M2-SC and M3-SC; in sample M1-SC these peaks are superposed with other wider reflection peaks. Moreover, in sample

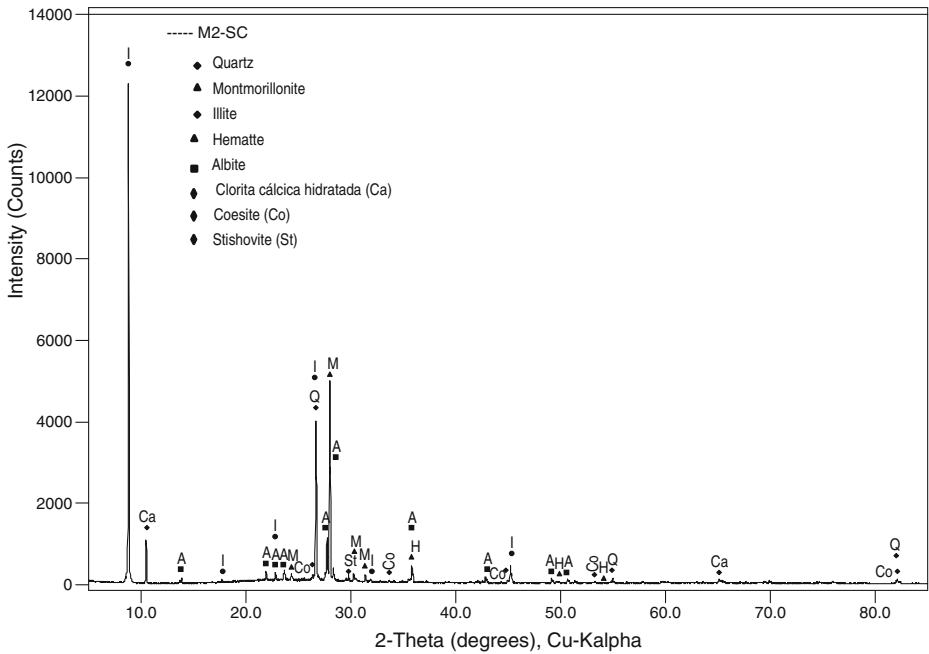


Fig. 4 X ray pattern for the sample M2-SC from the Carancas crater showing reflections of: Illite (I), Quartz (Q), Albite (A), Montmorillonite (M), Hematite (H), Hydrated Calcic Chlorite (Ca), Coesite (Co), and Stishovite (St)

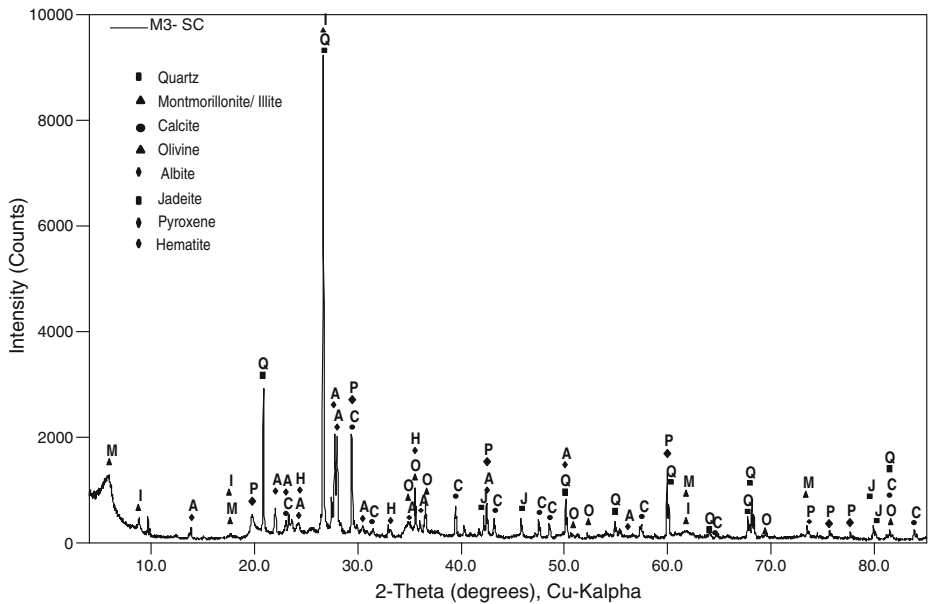


Fig. 5 X ray pattern for the sample M3-SC from the Carancas crater showing reflections of: Quartz (Q), Montmorillonite (M), Illite (I), Calcite (C), Olivine (O), Albite (A), Jadeite (J) Hematite (H) and Pyroxene (P)

Table 2 Hyperfine parameters of the Carancas meteorite samples

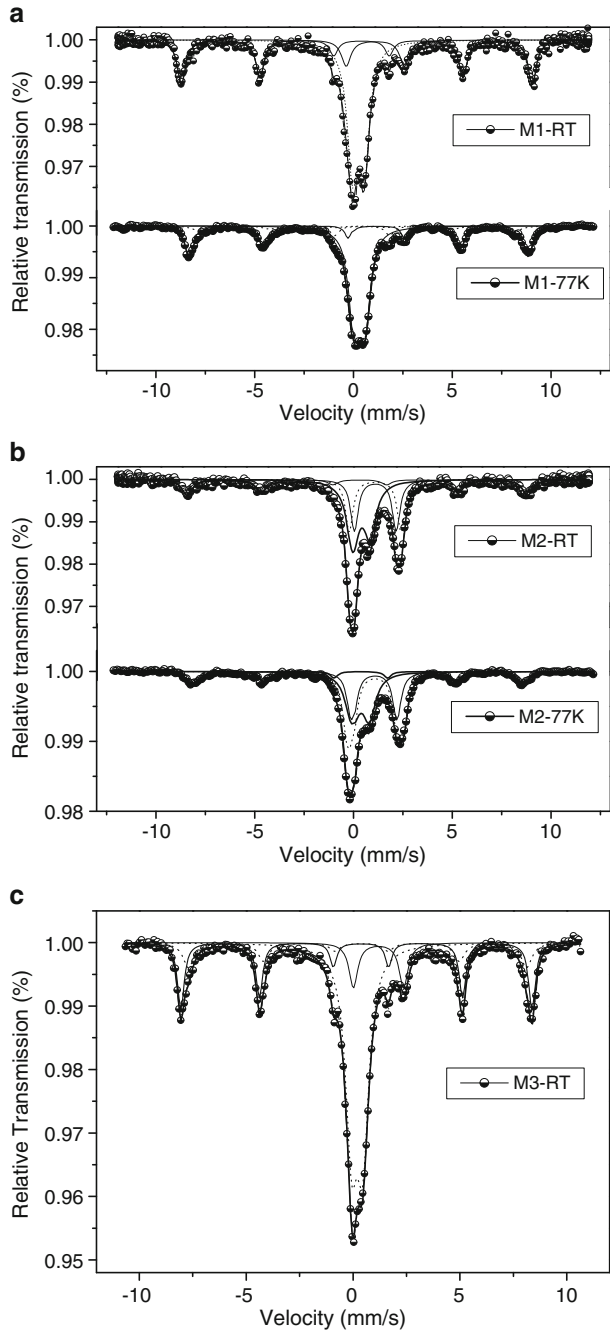
Mineral phases	Spectra taken at 298 K			
	δ (mm/s) ± 0.01	2ε (mm/s) ± 0.01	B_{hf} (T) ± 0.1	R. A. (%)
	M1-SC			
Doublet (Fe^{3+}), includes super paramagnetism	0.22	0.55		55
Hematite (Fe^{3+})	0.26	-0.22	50.8	35
Montmorillonite (Fe^{2+})	1.02	2.72		11
	M2-SC			
Illite (Fe^{3+})	0.35	0.85		35
Hematite (Fe^{3+})	0.23	-0.12	49.3	22
Illite (Fe^{2+})	1.00	2.47		11
Illite (Fe^{2+})	1.03	2.00		33
	M3-SC			
Hematite I (Fe^{3+})	0.30	-0.18	49.1	13
Hematite II (Fe^{3+})	0.27	-0.22	50.9	23
Illite (Fe^{3+}) /Montmorillonite	0.19	0.55		54
Olivine	1.22	2.30		9
	Spectra taken at 77 K			
	δ (mm/s) ± 0.01	2ε (mm/s) ± 0.01	B_{hf} (T) ± 0.1	R. A. (%)
	M1-SC			
Goethite	0.46	-0.20	49.4	8
Hematite (Fe^{3+})	0.51	-0.17	53.1	31
Montmorillonite (Fe^{3+})	0.46	0.49		56
Montmorillonite (Fe^{2+})	1.30	2.76		5
	M2-SC			
Illite (Fe^{3+})	0.49	0.82		35
Hematite (Fe^{3+})	0.43	-0.18	51.2	17
Illite (Fe^{2+})	1.24	2.85		17
Illite (Fe^{2+})	1.19	2.26		30

δ : isomer shift, 2ε : quadrupole shift, B_{hf} : hyperfine field, RA = relative area

M1-SC we observe the mineralogical phases of goethite and jadeite; in sample M3-SC we observe the presence of the following phases; quartz, interstratified montmorillonite-illite, calcite, olivine, albite, pyroxene and jadeite; the latter, which occurs also in sample M1-SC, is a pyroxene. Under high pressure, albite may be transformed to an association of jadeite + quartz [9], which could have happened when the meteorite collided with the soils of Carancas due to the powerful shock wave. In the sample M2-SC, we observe the presence of eight primary phases associated to well defined reflection peaks of illite, albite (without the presence of jadeite as compared with the sample M1-SC), quartz, montmorillonite, hematite, hydrated calcic chlorite, coesite and stishovite (Si_2O).

Silica, in the form of trigonal alpha-quartz, is one of the most common and resistant components of the crust of the Earth. During a powerful meteoritic impact, two polymorphs denser than silica, monoclinic coesite and tetragonal stishovite, can form from quartz under pressures higher than 3 to 10 GPa [10]. Although coesite can

Fig. 6 **a** Mössbauer spectra of the Carancas crater sample M1-SC taken at RT and at 77 K. **b** Mössbauer spectra of the sample M2-SC taken at RT and LNT. **c** Mössbauer spectrum of the sample M3-SC taken at RT



form under conditions of extreme metamorphism deep within the Earth, these are not sufficient to produce stishovite; consequently, its formation in the Earth can only take place in sites of meteoritic impacts [11], under the required intense pressures, as can be observed for sample M2-SC (Fig. 4).

Table 2 lists the ^{57}Fe hyperfine parameters corresponding to the different sub-spectra for these soil samples from the crater taken at RT and LNT. As shown in Fig. 6a the spectrum taken at RT for sample M1-SC was fitted with a magnetic sextet, assigned to an Fe^{3+} site, which is characteristic of hematite, and two paramagnetic doublets. The doublet with the largest area is assigned to an Fe^{3+} site, which may include sites in a superparamagnetic state, and the second one to an Fe^{2+} site which is associated to montmorillonite. Results from the spectrum taken at LNT (see Fig. 6a) confirm the presence of a strong sextet of hematite along with a weak sextet of goethite with 8 % of relative area, which contributed to the Fe^{3+} doublet at RT; moreover, it shows the presence of two doublets associated with Fe^{3+} and Fe^{2+} sites in montmorillonite. It is interesting to observe that the quadrupole shift for hematite at 77 K is negative, typical of a hematite sample that has not undergone the Morin transition (MT); therefore, it remains in a weak ferromagnetic state.

In Fig. 6b we can observe the RT Mössbauer spectrum of the sample M2-SC; it shows one magnetic sextet assigned to hematite, with $B_{\text{hf}} = 49.31$ T and three doublets, all of them assigned to illite, in agreement with the respective diffractogram, one of them associated to an Fe^{3+} site and two to Fe^{2+} sites. At LNT we observe that the above assignments are confirmed; we note that that the parameter B_{hf} of hematite increases with decreasing temperature and that the relative areas for the observed sites remain about the same at both temperatures.

In Fig. 6c we can observe the RT Mössbauer spectrum for the sample M3-SC; it shows two magnetic sextets both assigned to sites in hematite, with $B_{\text{hf}} = 50.9$ T and 49.1 T respectively; the latter corresponds to a hematite with substitution of Fe by Al, which is responsible for the decrease of the B_{hf} value; it shows also two doublets, one of them associated with Fe^{3+} in the montmorillonite structure, and the second one may be assigned to an Fe^{2+} site in olivine. We have no data at LNT.

4 Conclusions

The analyses of the crater soil samples by EDXRF reveal that they contain: Al, Si, S, Cl, K, Ca, Ti, Mn, Fe, Cu, Zn, Rb, and Sr; Al, S, Rb, Sr, and Cu are observed in about the same concentrations in the three samples; Ni is observed only in samples M1 y M3. The concentration of Si, Ca, and Ti in these samples are found to be higher than in the meteorite; the concentration of Si is found in the following relationship $\text{M1} > \text{M3} > \text{M2}$, Cl as $\text{M3} > \text{M1} > \text{M2}$, K as $\text{M1} > \text{M2} > \text{M3}$, Ca as $\text{M3} > \text{M2} > \text{M1}$; Fe as $\text{M1} > \text{M3} > \text{M2}$. The lower concentrations of Si, Cl and Fe in the sample M2-SC may be the result of the meteoritic impact.

The analyses by XRD show that the samples contain mineralogical phases consisting mainly of quartz (SiO_2), montmorillonite, illite, albite ($\text{NaAlSi}_3\text{O}_8$), and hematite, an iron oxide that is generally found in soils used for agricultural production. In the samples M1-SC and M3-SC it is observed the occurrence of jadeite; under high pressure albite decomposes to form the jadeite-quartz association, which could have happened when the meteorite collided with the soils at Carancas due to the powerful shock wave. In sample M2-SC, by XRD, we observe the presence of a high concentration of illite, and the characteristic peaks of impactites such as coesite and stishovite which are high pressure mineral polymorphs. These are generated by shock waves and up to now have only been identified in quartz containing rocks that

have suffered impact induced metamorphism within craters produced by meteorites. It is known that coesite can form under extreme metamorphic conditions within the crust of the Earth; however, these conditions are not sufficient to produce stishovite. Therefore, its formation on Earth can only take place in sites that were subjected to meteorite impacts. In sample M3-SC we observe main phases assigned to olivine and pyroxene, which are common minerals in meteorites and igneous rocks; taking as reference earlier studies we may assume that these minerals were ejected outside the crater and may constitute small fragments of the meteorite.

The analysis by TMS at RT and TNL allowed the observation of superposed magnetic, paramagnetic and superparamagnetic phases. The presence of hematite is evident in all samples. In the sample M1-SC at RT we identified super paramagnetic goethite, which at LNT becomes magnetically ordered goethite. The Fe^{3+} cations present in this sample are distributed in the octahedral sites of montmorillonite and part in goethite. In samples M1-SC and M2-SC hematite does not exhibit the Morin transition (MT) when cooled down to LNT. In the case of the sample M3-SC, its TMS spectrum taken at RT shows two magnetic sextets assigned to the presence of Fe^{3+} cations: one assigned to well crystallized hematite, and the other to hematite with Al substitution in Fe sites that causes a reduction of the observed magnetic hyperfine field.

Acknowledgements The authors are grateful for the collaboration of the Laboratories of Soil Analysis and Archaeometry at San Marcos University for allowing us the use of their instruments and materials; likewise, we are grateful to Dr. J. M. Grensch for providing the Mössbauer spectra taken at LNT in his laboratory at the Institut des Molécules et Matériaux du Mans (IMMM), Université du Maine, France.

References

- Loayza, M.L.C., Cabrejos, J.A.B.: *Hyperfine Interact.* **203**(1–3), 17–23 (2011)
- Langenhorst, F.: Shock metamorphism of some minerals: basic introduction and microstructural observations. *Bull. Czech. Geol. Surv.* **77**(4), 265–282 (2002)
- Langenhorst, F., Deutsch, A.: *Adv. Mineral.* **3**, 95–110 (1998). Springer-Verlag
- Wackerle, J.: Shock-wave compression of quartz. *J. Appl. Phys.* **33**, 922 (1962)
- Kieffer, S.W., Phakey, P.P., Christie, J.M.: *Contrib. Mineral. Petrol.* **1**(59), 41–93 (1976)
- Holland, K.G., Ahrens, T.J.: Melting of $(\text{Mg,Fe})_2\text{SiO}_4$ at the core-mantle boundary of the Earth. *Science* **275**, 1623–1625 (1997)
- Brand, R.A.: Normos-90 Mössbauer Fitting Program Package. U. of Duisburg, Alemania (1994)
- Cerón Loayza, M.L., Bravo Cabrejos, J.A.: Caracterización Mineralógica de un Impacto Meteorítico en la Localidad de Carancas–Puno. *Rev. Investig. Fis.* **12**(1), 5–12 (2009)
- Vanderberghe, R.E., De Grave, E., De Geyter, G., Landuydt, C.: *Clays Clay Miner.* **34**(3), 275–280 (1986)
- Hemley, R.J., Prewitt, C.T., Kingma K.J.: High pressure behavior of silica. *Rev. Mineral.* **29**, 41–82 (1994)
- Chao, E.C.T., Fahey, J.J., Littler, J., Milton D.J.: Stishovite, SiO_2 , a very high pressure new mineral from meteor crater, Arizona. *J. Geophys. Res.* **67**(1), 419–421 (1962)